Int. J. Environ. Sci. Technol. (2016) 13:113–124
DOI 10.1007/s13762-015-0827-9

ORIGINAL PAPER

Preparation of amino functionalized imidazolium-modified silicas by different coupling agents for removal of 2,4-dinitrophenol from aqueous solutions

Z. Wang[1] · C. Ye[2] · H. Wang[2]

Received: 5 May 2014 / Revised: 3 April 2015 / Accepted: 26 April 2015 / Published online: 6 May 2015

Abstract Amino group exhibits alkaline properties. Amino functionalized imidazole-modified silicas would benefit the adsorption of phenolic compounds. Coupling agent between the silica and the imidazolium ring has an effect on adsorption performance. In this paper, two adsorbents were synthesized for the surface bonding of *N*-(3-aminopropyl)-imidazole onto silicas modified by 3-chloropropyltriethoxysilane and 3-mercaptopropyltrimethoxysilane, respectively. Infrared spectra, elemental analysis, thermogravimetric analysis and N_2 adsorption–desorption isotherms were used to characterize the two adsorbents, and their adsorption capacities of 2,4-dinitrophenol from aqueous solutions were investigated in detail. The experimental results indicated that amino group plays an important role in the enhancement of adsorption capacities of 2,4-dinitrophenol. The adsorbent with 3-mercaptopropyltrimethoxysilane as coupling agent exhibited lower adsorption capacity due to a weak electron–electron repulsion between the non-bonding electrons of sulfur atom and π electrons of benzene ring of 2,4-dinitrophenol. The adsorption kinetics fitted well with pseudo-second-order model. The two adsorbents could be regenerated and reused eight times at least by washing with HCl. The adsorption mechanism was also discussed.

Keywords Adsorption · Desorption · Ionic liquids · Silica

Introduction

Phenolic compounds are widely used as intermediates in many industry fields such as petrochemicals, pharmaceuticals, pesticides, insecticides and plastics. (Duarte et al. 2014; Yang et al. 2014). Phenolic compounds appear in the list of priority pollutants of many countries due to their high toxicity and persistency in the environment even at low concentrations (Mehrizad et al. 2012; Pacurariu et al. 2013; Chaudhary and Balomajumder 2014). Therefore, effective treatment of wastewaters containing these chemicals should be required before safe discharge into water bodies.

Up to now, various methods such as catalytic oxidation, photooxidation, electrochemical oxidation, ultrafiltration and adsorption have been proposed to remove phenolic compounds from wastewater (Wiśniewski et al. 2012; Zhang et al. 2012; Feng et al. 2015; Ayusheev et al. 2014; Hurwitz et al. 2014). Among these proposed methods, adsorption is an effective method for the removal of phenolic compounds from wastewater due to its simplicity and easy operation process. A variety of adsorbents were used to remove phenolic pollutants from wastewater including activated carbon (Yang et al. 2014), fly ash (Srivastava et al. 2006; Chaudhary and Balomajumder 2014), polymers (Huang et al. 2013; Pacurariu et al. 2013), mesoporous sieves (Fu et al. 2011), chitosan (Zhou et al. 2014), zeolites (Yousef et al. 2011) and silica (Qin et al. 2013). Lorenc-Grabowska et al. (2013) reported that the adsorption

Electronic supplementary material The online version of this article (doi:10.1007/s13762-015-0827-9) contains supplementary material, which is available to authorized users.

✉ Z. Wang
wzk@htu.cn

[1] School of Environment, Henan Key Laboratory for Environmental Pollution Control, Key Laboratory for Yellow River and Huai River Water Environment and Pollution Control, Ministry of Education, Henan Normal University, Xinxiang 453007, China

[2] School of Chemistry and Chemical Engineering, Henan Normal University, Xinxiang 453007, China

performance is related to the structure of the adsorbent (i.e., porous texture, surface chemistry), the properties of the adsorbate (i.e., molecular size, solubility, pK_a, physicochemical properties) and the operational conditions (i.e., pH, temperature). Phenolic pollutants are a kind of weak acids with aromatic properties. Moreover, oxygen atom of phenolic hydroxyl groups has lone pair electrons. Therefore, one or more of three interactions such as π–π dispersion force, electrostatic force and hydrogen bond should be considered during the adsorption of phenolic compounds (Velasco and Ania 2011; Liu et al. 2014). As a consequence, the adsorbents with surface basic characteristics, surface atoms with the ability to form hydrogen bond and delocalized π-electrons should be suitable for the removal of phenolic pollutants.

Ionic liquid-modified silicas have combined some of the advantages of both ionic liquids and supports of silica. Usually, there are two methods to prepare this kind of materials, which immobilize ionic liquids via simple wet impregnation method or covalent grafting method. Recently, these materials are used as catalysts (Vafaeezadeh and Hashemi 2014), chromatography stationary phases (Zhang et al. 2014), solid phase extraction adsorbents (Vidal et al. 2012a, b) and removal of various pollutants from aqueous solutions such as mercury, lead, thiophenic sulfur compounds and 2,4-dinitrophenol (2,4-DNP) (Mahmoud 2011; Mahmoud and Al-Bishri 2011; Sun et al. 2013; Wang et al. 2013a, b).

In order to achieve the targeted application, ionic liquid-modified silicas can be tailored by using the "designer solvents" of ionic liquids. Imidazole, which has a planar 5-membered ring, appears to be aromatic due to the presence of a sextet of π-electrons (π_5^6). As an amphoteric substance, the alkalinity of imidazole is sixty times that of pyridine (p$K_b \approx 7$). These properties of imidazole (i.e., π–π dispersion interaction, surface basic characteristic) would make imidazole-modified silicas remove phenolic pollutants from aqueous solutions easily. Amino group is easily protonated under acidic conditions and also contributes to the basic properties, so the surface basicity of imidazole-modified silicas will be further enhanced when amino group is grafted onto imidazole through alkyl chain. For example, amination of activated carbon showed an outstanding enhancement of phenol adsorption (Arrigo et al. 2010; Yang et al. 2014). Generally, ionic liquid-modified silicas are composed of cations, anions and coupling agents between silica and imidazole. The structures of cations, anions and coupling agents should have a significant effect on the characteristics of these materials (Han et al. 2012; Kotadia and Soni 2012; Mousavi and Pawliszyn 2013; Maroneze et al. 2014; Zhu et al. 2014). However, little is known about the effect of amino group and coupling agent to the adsorption capacity of imidazole-modified silicas. In this work, *N*-(3-aminopropyl)-imidazoles were covalently attached onto the surface of bare silicas using 3-chloropropyltriethoxysilane and 3-mercaptopropyltrimethoxysilane as coupling agents. The obtained adsorbents were 1-alkyl-3-(propyl-3-amino) imidazolium-modified silica (SilprP_3NImBr) and 1-allyl-3-(propyl-3-amino) imidazolium-modified silica (SilprSP_3NImBr). A special emphasis was placed on the adsorption behaviors of 2,4-DNP from aqueous solutions onto the two adsorbents, and the mechanism was also discussed.

This study was conducted from May 2012 to November 2013 in the School of Environment, Henan Key Laboratory for Environmental Pollution Control, Key Laboratory for Yellow River and Huai River Water Environment and Pollution Control, Ministry of Education, Henan Normal University, Xinxiang, China.

Materials and methods

Materials and reagents

Silica gel (200–300 mesh), 3-bromopropylamine hydrobromide (98 %), 1-allylimidazole (97 %), azodiisobutyronitrile (AIBN) and 2,4-DNP were obtained from Sinopharm Chemical Reagent Co., Ltd. Imidazole (99 %), 3-chloropropyltriethoxysilane (98 %) and 3-mercaptopropyltrimethoxysilane (95 %) were purchased from Aladdin Chemistry Co. Ltd. All solvents such as acetone, diethyl ether, toluene, acetonitrile, methanol and ethanol were of analytical grade. Toluene was purified by the following procedure: Toluene was firstly dried with calcium chloride, and then was further dried by standing with sodium. Finally, anhydrous toluene was obtained by distillation.

Synthesis of ionic liquid-modified silica

Synthesis of SilprP_3NImBr

Silica was first immersed in 6 mol/L hydrochloric acid for 24 h. Then, it was washed with doubly distilled water (DDW) until pH was neutral. The activated silica was obtained by drying at 60 °C for 12 h (Vidal et al. 2012a, b). The aim of pretreatment is to enhance the content of silanol groups on the silica surface and to remove metal oxide. The immobilized ionic liquids were synthesized according to literature (Tian et al. 2013) with some modification. Five grams of the activated silica was suspended in 50.0 mL dry toluene, and then, an excess of 3-chloropropyltriethoxysilane (5.0 mL) was added. The suspension was refluxed for 24 h. After that, the reaction was stopped and the modified

silica was cooled to room temperature and washed in turn with toluene, DDW and methanol. Chloropropyl silica, SilprCl, was dried at 60 °C for 10 h.

Second, the chemically bonded chloropropyl groups on the silica surface were subsequently reacted with imidazole. In brief, 5.0 g dry SilprCl was added into a reaction flask containing 50.0 mL dry toluene and a large excess of imidazole (5.0 g). After refluxing with stirring for 24 h, the modified silica was cooled to room temperature and washed in turn with toluene, ethanol and methanol. The silica chemically bonded with imidazole, SilprImCl, was dried at 60 °C for 10 h.

Third, 5.0 g SilprImCl was placed in a 250-mL round-bottom flask with 100.0 mL ethanol and 4.0 g 3-bromopropylamine hydrobromide. The suspension was then refluxed with stirring for 24 h. After washing with ethanol and drying at 60 °C for 10 h, the 1-alkyl-3-(propyl-3-amino) imidazolium-modified silica, SilprP_3NImBr, was obtained. The preparation procedure is schematically shown in Fig. S1 (1) (see supplementary material).

Synthesis of SilprSP_3NImBr

7.5 g of the activated silica was suspended in 100.0 mL of dry toluene, and then, an excess of 3-mercaptopropyltrimethoxysilane (8.0 mL) was added in a 250-mL round-bottom flask. The suspension was stirred and refluxed for 24 h. After refluxing, the reaction was stopped and the modified silica was cooled to room temperature and washed in turn with toluene, anhydrous ethanol, DDW and acetone. 3-Mercaptopropyl silica, SilprS, was dried at 60 °C for 10 h (Qiu et al. 2009).

To a 250-mL round-bottom flask, 3.0 g of SilprS, 50.0 mL acetonitrile, 3.0 g 1-allylimidazole and 0.3 g AIBN were added successively. Then, the mixture was stirred and refluxed 12 h. The precipitate was filtered and washed with solvents in the order of acetonitrile, acetone and diethyl ether. The mercaptopropyl silica bonded with imidazole, SilprSIm, was dried at 60 °C for 10 h.

Finally, 5.0 g SilprSIm was placed in a 250-mL flask with 100.0 mL ethanol and 4.0 g 3-bromopropylamine hydrobromide. The suspension was then refluxed with stirring for 24 h. After washing with ethanol and drying at 60 °C for 10 h, the 1-allyl-3-(propyl-3-amino) imidazolium-modified silica, SilprSP_3NImBr, was obtained. The synthetic procedure is shown in Fig. S1 (2) (see supplementary material).

Characteristic analysis

The Fourier transform infrared (FT-IR) data were obtained using a Perkin-Elmer 983 IR spectrophotometer over the wave number range 400–4000 cm^{-1}. A KBr pellet was used for analysis. Thermogravimetric analysis (STA449C, Netzsch, Germany) was performed with a heating rate of 10 °C/min under nitrogen. The carbon, hydrogen and nitrogen of all the intermediates and final materials were determined by elemental analysis that performed on a Vario EL elemental analyzer (Germany). Two parallel analyses were made for each material. The porosity characteristics of SilprP_3NImBr and SilprSP_3NImBr were investigated by N_2 adsorption–desorption experiments on a Quantachrome NOVA 2000e sorption analyzer at liquid nitrogen temperature (77 K). The specific surface area (S_{BET}) was estimated by the linear part of the Brunauer–Emmett–Teller (BET) equation (Ladavos et al. 2012), and the pore size distribution was calculated from the adsorption branch of the isotherms by the Barrett–Joyner–Halenda (BJH) method (Barrett et al. 1951).

Static adsorption

Batch adsorption experiments were used to investigate the interactions between ionic liquid-modified silica adsorbents and 2,4-DNP. 1 mol/L HCl or 1 mol/L NaOH were used for pH adjustment using a shanghai pHs-2 pH meter fitted with a combination glass electrode. 2,4-DNP solutions ($V = 50.00$ mL, $C_0 = 50$ mg/L) were shaken at 160 rpm in a 100-mL conical flask with a predetermined amount of adsorbents for various times at constant temperature using a THZ-82(A) thermostatic water-bath shaker (Jintan Scientific Analytical Instrument Co. Ltd., China). After shaking, the mixtures were filtrated using filter paper and the 2,4-DNP concentrations were measured using a UV/visible spectrophotometer (UV-5100,Shanghai Metash Instruments Co., Ltd, China). The adsorption capacity of 2,4-DNP in mg/g was calculated by the following Eq. (1).

$$Q = \frac{V(C_0 - C_t)}{W} \quad (1)$$

where C_0 (mg/L) and C_t (mg/L) are the liquid phase concentrations of 2,4-DNP at initial and at time t, respectively. V (L) is the volume of the solution, and W (g) is the mass of dry imidazole-modified silicas added.

Dynamic adsorption, elution and reuse

Two hundred and fifty milligrams of SilprP_3NImBr or SilprSP_3NImBr was packed into empty polypropylene cartridges with the length of 66 mm and an inner diameter of 12.7 mm, which were purchased from Shenzhen Biocomma Biotech Co., Ltd. Then, the cartridges were pretreated with 10 mL methanol and 10 mL DDW in turn. 250 mL of 0.2 mg/L 2,4-DNP aqueous solutions with pH 4.0 were uploaded onto a cartridge at a flow rate of 1 mL/min. 2,4-DNP was eluted by different concentrations and

volumes of HCl after washing with 10 mL DDW. In order to determine the reusability of the two adsorbents, consecutive adsorption–elution cycles were repeated eight times by using the same adsorbent.

Results and discussion

Characterization

IR spectroscopy

The spectra of silica, SilprCl, SilprImCl, SilprP_3NImBr, SilprS, SilprSIm and SilprSP_3NImBr were recorded between 400 and 4000 cm^{-1} as shown in Fig. S2 (see supplementary material). The spectra of O–H vibration at 3450 and 1631 cm^{-1} were attributed to the physical adsorbed water and the typical peaks of Si–O–Si could also be observed around 796 and 1090 cm^{-1}. For the silica, an absorption peak at around 950 cm^{-1} means the presence of silanol groups (Vidal et al. 2012a, b). For the SilprCl, a conspicuous peak at 700 cm^{-1} indicated the presence of C–Cl group, which belong to the finger print region of C–Cl vibration ranging from 690 to 704 cm^{-1} (Bi and Row 2010). In the spectra of SilprImCl and SilprP_3NImBr, the peak at 700 cm^{-1} disappeared, which indicated the imidazole was reacted with SilprCl and the chlorine was replaced by imidazole (Tian and Row 2011). The imidazole group was indicated by the characteristic imidazole peaks at 1519 and 1573 cm^{-1}. These results showed that SilprCl, SilprImCl and SilprP_3NImBr were synthesized successfully.

In the spectra of SilprS, SilprSIm and SilprSP_3NImBr, the characteristic peak at 685 cm^{-1} was assigned to the C–S stretch (Khdary et al. 2014). The characteristic peak at 2930 cm^{-1} was attributed to the C-H stretching of the tetrahedral carbon. For the SilprSIm and SilprSP_3NimBr, the peaks at 1521 and 1547 cm^{-1} were attributed to the characteristic frequency of the imidazolium groups, which confirmed the immobilization of imidazole onto silica was successful (Qiu et al. 2010).

Thermogravimetric analysis

The thermogravimetric curves give the information of the thermal stability of the chemically modified silicas and can be also employed to determine the amount of the compounds immobilized, since the weight loss from 200 to 800 °C was associated with the loss of the organic groups attached to the surface (Bi and Row 2010). It can be seen from the Fig. S3 (see supplementary material) that there is an initial loss of weight at a temperature below 100 °C for all samples. This is attributed exclusively to the removal of adsorbed water molecules, which could be removed completely by further heating to about 200 °C. Figure S3 (1) shows the thermogravimetric curves of SilprCl, SilprImCl and SilprP_3NimBr. From 200 to 800 °C, it presents 14.37, 15.00 and 21.07 % mass loss for SilprCl, SilprImCl and SilprP_3NimBr, respectively. For the SilprS, SilprSIm and SilprSP_3NimBr, as shown in Fig. S3 (2), 13.90, 16.44 and 22.17 % mass losses were observed, respectively. It was evident that the imidazole-modified silicas presented an even higher mass loss than that of the SilprCl or SilprS in the temperature range of 200–800 °C. Hence, it could be concluded that the immobilization of amino group and imidazole onto silica was successful.

Elemental analysis

Table S1 (see supplementary material) lists the carbon, hydrogen and nitrogen elemental content and the surface coverages of SilprCl, SilprImCl, SilprP_3NImBr, SilprS, SilprSIm and SilprSP_3NImBr. According to the reference (Bi and Row 2010), the surface coverages were calculated according to the following equations:

$$\text{Surface coverage}\,(\mu\text{mol}/\text{m}^2) = \frac{\%\text{C}}{36 \times (1 - \%\text{C} - \%\text{H}) \times S} \quad (2)$$

$$\text{Surface coverage}\,(\mu\text{mol}/\text{m}^2) = \frac{\%\text{N}}{28 \times (1 - \%\text{C} - \%\text{H} - \%\text{N}) \times S} \quad (3)$$

$$\text{Surface coverage}\,(\mu\text{mol}/\text{m}^2) = \frac{\%\text{N}}{42 \times (1 - \%\text{C} - \%\text{H} - \%\text{N}) \times S} \quad (4)$$

where *%C*, %H and %N represent the percentages of carbon, hydrogen and nitrogen, respectively, as determined by elemental analysis shown in Table S1, and *S* is the specific surface area of the silica support (605 m^2/g, BET). The surface coverages of SilprCl and SilprS were calculated according to Eq. (2) based on the percentage amounts of carbon. The surface coverages of SilprImCl and SilprSIm were calculated according to Eq. (3) based on the percentage amounts of nitrogen. The surface coverages of SilprP_3NImBr and SilprSP_3NImBr were calculated according to Eq. (4) based on the percentage amounts of nitrogen. The elemental analysis data proved that immobilization on the surface was successful.

N_2 adsorption–desorption isotherms

Figures S4 and S5 (see supplementary material) show the N_2 adsorption–desorption isotherms and the average pore size distributions of SilprP_3NImBr and SilprSP_3NImBr. As

can be seen in Fig. S4, the N_2 adsorption–desorption isotherms were Type IV according to the IUPAC classification (Guo et al. 2013). The pore size distribution curves of $SilprP_3NImBr$ and $SilprSP_3NImBr$ in Fig. S5 show a narrow unimodal distribution centered at 3–4.5 and 4–5.5 nm, respectively. The corresponding physical properties including BET surface area, pore size and pore volume were also given in Table S2 (see supplementary material).

Reproducibility of adsorption experiments

In order to test reproducibility of the adsorption experiments, ten parallel experiments were carried out with the two adsorbents, respectively. The experimental conditions are initial concentration 50 mg/L, pH 4.0, adsorbent dosage 25 mg, shaking speed 160 rpm, shaking time 180 min and temperature 30 °C. The adsorption capacity of 2,4-DNP onto the $SilprP_3NImBr$ was 59.02, 58.88, 58.93, 59.76, 58.59, 60.13, 60.42, 60.28, 58.91 and 59.81 mg/g, respectively. The adsorption capacity of 2,4-DNP onto the $SilprSP_3NImBr$ under the same experimental conditions was 45.65, 46.75, 45.89, 46.78, 46.94, 45.82, 47.02, 45.89, 45.96 and 45.97 mg/g, respectively. The results indicated that relative standard deviation for the ten parallel experiments did not exceed 1.5 %.

Effect of pH

The pH of the solutions containing 2,4-DNP may affect the surface charge of the $SilprP_3NImBr$ or $SilprSP_3NImBr$ adsorbents through the protonation of the aminopropyl group and the degree of ionization, solubilization and the existing form of 2,4-DNP in aqueous solutions (Vidal et al. 2012a, b). Therefore, the pH of the solutions plays an important role in the adsorption of 2,4-DNP. The effect of pH on 2,4-DNP adsorption was determined for different pH values ranging from 2.0 to 10.0 at initial concentration 50 mg/L, shaking speed 160 rpm, shaking time 180 min and temperature 30 °C. As shown in Fig. 1, the adsorption capacity of 2,4-DNP onto $SilprP_3NImBr$ or $SilprSP_3NImBr$ increased significantly with an increase in pH from 2.0 to 4.0 and maintained a stable value in the pH range of 4.0–9.0. When the pH of the solution is further increased, the adsorption capacity of 2,4-DNP onto $SilprP_3NImBr$ or $SilprSP_3NImBr$ decreased significantly at pH 10.0. In addition, it is interesting that the adsorption capacities of 2,4-DNP onto $SilprP_3NImBr$ were larger than those of 2,4-DNP onto $SilprSP_3NImBr$ over the wide pH conditions ranging from 4.0 to 9.0, which may be attributed to the difference of the coupling agents between the $SilprP_3NImBr$ and the $SilprSP_3NImBr$. For the

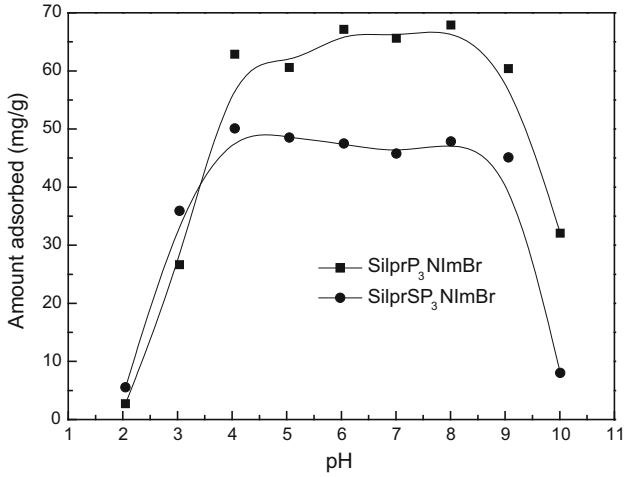

Fig. 1 Effect of pH on the adsorption of 2,4-DNP on $SilprP_3NImBr$ and $SilprSP_3NImBr$

$SilprP_3NImBr$, the linker was propyl, while the linker was propyl sulfide for the $SilprSP_3NImBr$, and the sulfur atom forms a σ bond with each carbon atom of its neighbors. The remaining two pairs of lone pair electrons of the sulfur have a weak electron–electron repulsion with π electrons of benzene ring of 2,4-DNP, resulting in the low adsorption capacity of 2,4-DNP.

In order to account for the effect of pH, we need to clarify the type of interaction between 2,4-DNP and the two adsorbents. The pK_a value of 2,4-DNP is 3.96, indicating that the major species of 2,4-DNP in the solutions is in a neutral molecule at the pH value below 3.96 and in an anionic form at the pH value above 3.96. It is widely recognized that imidazole-modified silicas are anion-exchangeable material (Zhang et al. 2014). In the pH range of 2.0–4.0, anion-exchange interactions played an important role between the two adsorbents and 2,4-DNP. A large amount of the neutral molecules of 2,4-DNP in the solutions would prevent the anion-exchange reactions leading to their lower adsorption capacity for 2,4-DNP. The pK_a value of aminopropyl group is 9.8, and the aminopropyl groups are positively charged by protonation at pH lower than 9.8. $SilprP_3NImBr$ and $SilprSP_3NimBr$ not only have the large organic cation imidazolium, but also contain the aminopropyl groups to strengthen the electrostatic interaction by the protonation of amino group. Thus, besides anion-exchange interaction, there was an additional electrostatic interaction between the 2,4-DNP anions and the two adsorbents due to a great amount of 2,4-DNP anions and the protonation of amine group. The double interactions existed between the two adsorbents, and 2,4-DNP resulted in higher 2,4-DNP adsorption capacity in the range of 4.0–9.0. However, at pH above 9.8, increasing solution pH decreased

the degree of protonation of aminopropyl group, which could greatly decrease the electrostatic interaction between the 2,4-DNP and adsorbents and decrease 2,4-DNP adsorption capacity. This meant that at pH above 9.0, the major interactions were still anion-exchange. On the other hand, the lower adsorption at high pH is probably due to the presence of excess OH^- ions competing with the 2,4-DNP anions for anion-exchange reactions. As a result, there was a significant reduction in the adsorption capacity of 2,4-DNP.

According to above discussions, the two adsorbents are of primary anion-exchange and electrostatic nature. Therefore, the presence of excess anions in solutions would affect the adsorption of 2,4-DNP. In order to further elucidate the adsorption mechanism, some commonly seen anions such as Cl^-, Br^-, NO_3^- and SO_4^{2-} were added into the solutions in the form of NaCl, NaBr, $NaNO_3$ and Na_2SO_4, respectively. The results are presented in Fig. 2. As can be seen from this figure, the adsorption capacity of 2,4-DNP onto $SilprP_3NImBr$ and $SilprSP_3NImBr$ decreased significantly with increasing the concentration of anions from 0 to 0.1 mol/L.

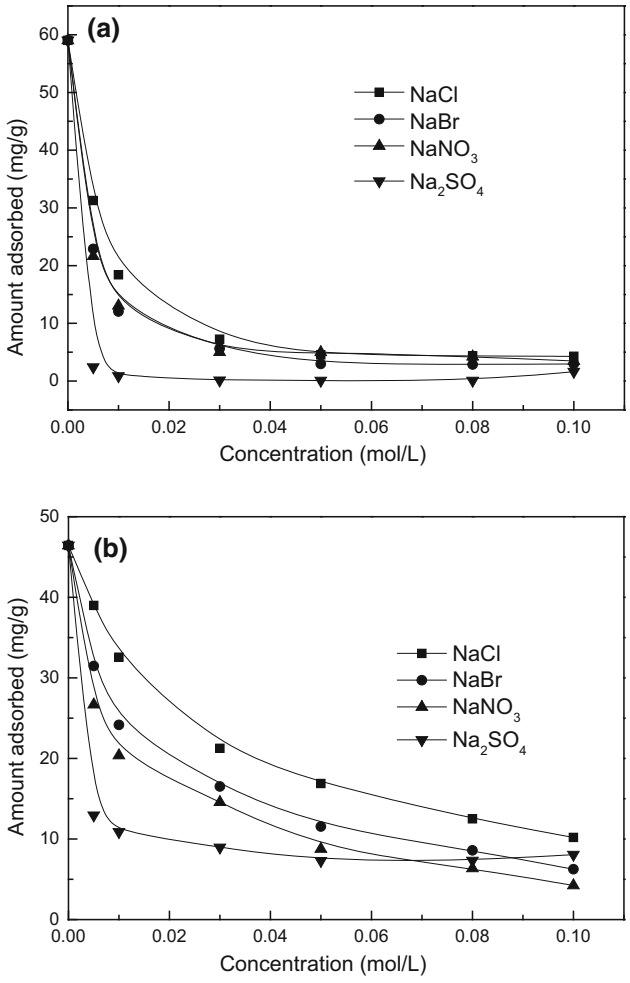

Fig. 2 Effect of anion concentration on the adsorption of 2,4-DNP on $SilprP_3NImBr$ (**a**) and $SilprSP_3NImBr$ (**b**)

Effect of initial concentration and adsorbent dosage

The effect of initial 2,4-DNP concentration on adsorption capacity onto the two adsorbents was investigated at pH 4.0, shaking speed 160 rpm, shaking time 180 min and temperature 30 °C. It is obvious from Fig. 3 that as the initial concentration increases from 5 to 50 mg/L, the equilibrium adsorption capacity also increases significantly. This may be attributed to the increase in the mass transfer driving force due to the increase in initial concentration. The effect of dosage of the two adsorbents was illustrated in Fig. 4; it can be seen from this figure that the amount of 2,4-DNP adsorbed per unit mass of adsorbent decreased with the increasing of adsorbent dosages. This may be attributed to the excessive adsorbent with the further increasing of adsorbent dosage. Generally, a series of adsorption isotherms are used to provide important information for elucidating the interaction of 2,4-DNP with the adsorbents. The most common models are Langmuir, Freundlich and Toth (Gimbert et al. 2008; Chao et al. 2014), and the linear form as shown in Eqs. (5), (6) and (7), respectively, were used to evaluate the adsorption experimental data provided from Fig. 3.

$$\frac{C_e}{Q_e} = \frac{C_e}{Q_m} + \frac{1}{bQ_m} \quad (5)$$

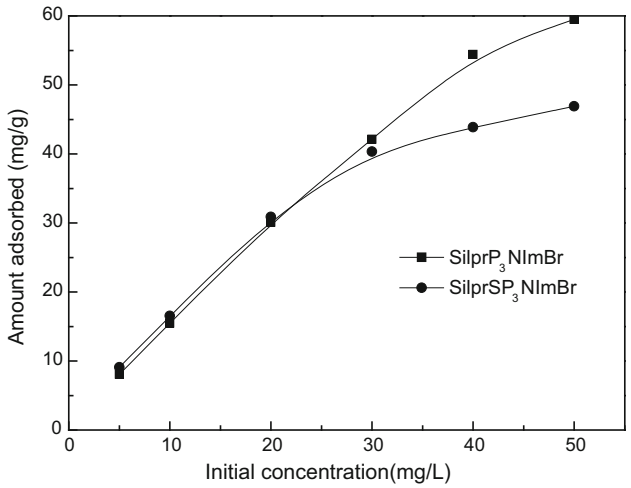

Fig. 3 Effect of initial concentration on the adsorption of 2,4-DNP

$$\ln Q_e = \ln K_F + \frac{1}{n}\ln C_e \quad (6)$$

$$\ln \frac{Q_e}{Q_{mt}} = \ln C_e - \frac{1}{m_t}\ln\left(K_t + C_e^{m_t}\right) \quad (7)$$

where C_e and Q_e are the equilibrium concentration (mg/L) and the equilibrium adsorption capacity (mg/g), respectively; Q_m is the monolayer adsorption capacity (mg/g); b is the Langmuir constant; K_F and $1/n$ are the constants indicative of the relative adsorption capacity of the adsorbent and the heterogeneity factor of Freundlich adsorption isotherm, respectively. Q_{mt} is the Toth maximum adsorption capacity (mg/g), m_t and K_t are the Toth constants.

The experimental results revealed that the Langmuir model was very suitable for describing the adsorption equilibrium of 2,4-DNP by the two adsorbents. The calculated values of the Langmuir, Freundlich and Toth constants and the correlation coefficients are listed in Table 1. As shown in Table 1, the values of 1/n which were less than 1.0 for the two adsorbents indicated that the adsorption of 2,4-DNP onto amino functionalized imidazolium-modified silicas was more favorable compared with our previously synthesized imidazole-modified silicas

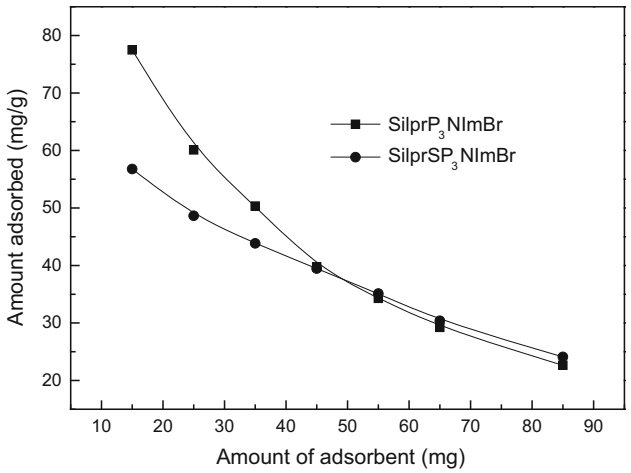

Fig. 4 Effect of amount of adsorbent on the adsorption of 2,4-DNP

Table 1 Langmuir, Freundlich and Toth isotherm constants

Adsorbents	Model	Parameter	
$SilprP_3NImBr$	Langmuir model	Q_m (mg/g)	91.74
		b (L/mg)	0.0972
		R^2	0.9868
	Freundlich model	K_F (mg/g) (mg/L)^n	8.9236
		$1/n$	0.6836
		R^2	0.9826
	Toth model	Q_{mt} (mg/g)	72.35
		m_t	1.5493
		K_t	34.56
		R^2	0.9915
$SilprSP_3NImBr$	Langmuir model	Q_m (mg/g)	51.81
		b (L/mg)	0.3386
		R^2	0.9973
	Freundlich model	K_F (mg/g) (mg/L)^n	13.6645
		$1/n$	0.4188
		R^2	0.9642
	Toth model	Q_{mt} (mg/g)	54.69
		m_t	0.8851
		K_t	2.6044
		R^2	0.9845

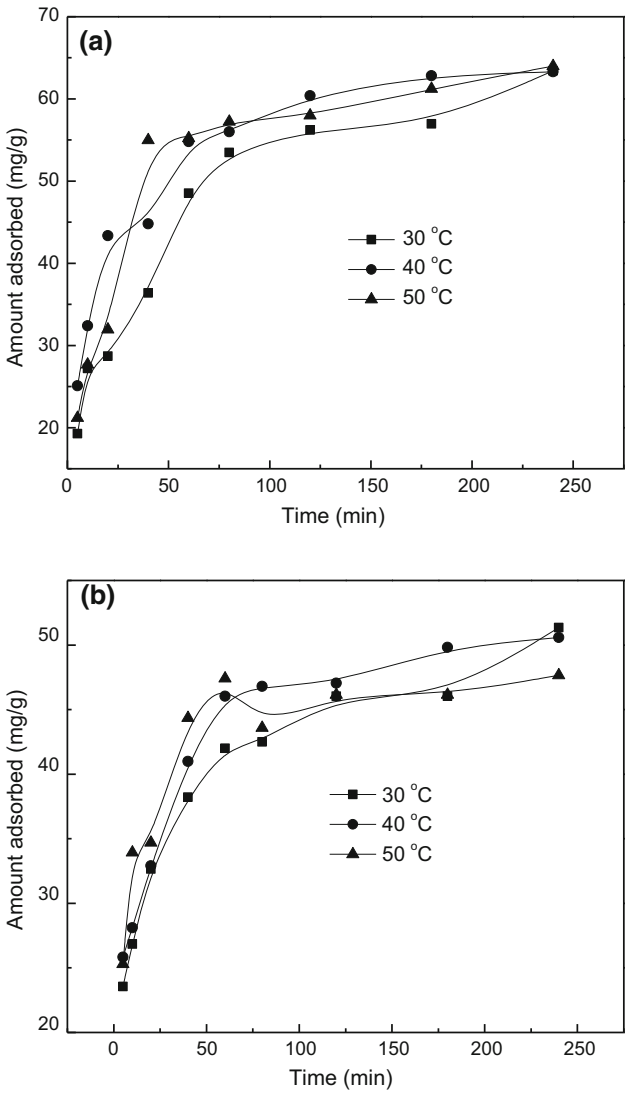

Fig. 5 Effect of shaking time on the adsorption of 2,4-DNP onto $SilprP_3NImBr$ (**a**) and $SilprSP_3NimBr$ (**b**)

Table 2 Kinetic parameters for the adsorption of 2,4-DNP on two adsorbents

Adsorbents	Model	Parameter	30 °C	40 °C	50 °C
$SilprP_3NImBr$		$Q_{e(exp)}$ (mg/g)	63.4	63.3	64.0
	Pseudo-first-order model	k_1 (1/min)	0.012	0.023	0.015
		$Q_{e(cal)}$ (mg/g)	38.6	40.6	31.8
		R^2	0.8845	0.9857	0.8414
		$P\%$	41.8		
	Pseudo-second-order model	k_2 (g/mg min)	0.007	0.0012	0.0010
		$Q_{e(cal)}$ (mg/g)	66.7	66.7	67.1
		h (mg/g min)	3.064	5.385	4.682
		R^2	0.9912	0.9985	0.9974
		$P\%$	5.14		
	Intraparticle diffusion model	k_3 (mg/g $min^{1/2}$)	3.297	2.788	3.148
		C (mg/g)	16.7	26.7	22.5
		R^2	0.9138	0.8637	0.7859
		$P\%$	9.53		
$SilprSP_3NImBr$		$Q_{e(exp)}$ (mg/g)	51.3	50.6	47.7
	Pseudo-first-order model	k_1 (1/min)	0.009	0.019	0.014
		$Q_{e(cal)}$ (mg/g)	22.3	22.9	9.2
		R^2	0.8614	0.9432	0.3466
		$P\%$	63.9		
	Pseudo-second-order model	k_2 (g/mg min)	0.0016	0.0021	0.0041
		$Q_{e(cal)}$ (mg/g)	51.8	52.1	48.1
		h (mg/g min)	4.203	5.663	9.569
		R^2	0.9945	0.9991	0.999
		$P\%$	1.59		
	Intraparticle diffusion model	k_3 (mg/g $min^{1/2}$)	1.949	1.917	1.408
		C (mg/g)	23.0	25.4	29.6
		R^2	0.9079	0.8442	0.6717
		$P\%$	6.84		

(Wang et al. 2013a, b). Therefore, amino groups that grafted onto the surface of imidazole-modified silicas led to an increase in the adsorption of 2,4-DNP.

Effect of time

Shaking time represents one of the significant contributing factors to the adsorption process when the batch equilibrium technique is utilized. The influence of shaking time on 2,4-DNP adsorption from aqueous solutions was determined for different temperature values ranging from 30 to 50 °C at initial concentration 50 mg/L, solution pH 4.0 and shaking speed 160 rpm using $SilprP_3NimBr$ and $SilprSP_3$-NimBr as adsorbent, respectively (Fig. 5). In order to further determine the mechanism of adsorption of 2,4-DNP onto the two adsorbents, the kinetic data shown on Fig. 5 were statistically investigated using the pseudo-first-order, pseudo-second-order and intraparticle kinetic models, as shown in Eqs. (8), (9) and (10), respectively (El-Sheikh 2014; Vala et al. 2014).

$$\ln (Q_e - Q_t) = \ln Q_e - k_1 t \tag{8}$$

$$\frac{t}{Q_t} = \frac{1}{Q_e^2 k_2} + \frac{t}{Q_e} \tag{9}$$

$$Q_t = k_3 \sqrt{t} + C \tag{10}$$

where Q_e and Q_t are the adsorption capacity at equilibrium and at time t, respectively (mg/g); k_1 (1/min), k_2 (g/mg min) and k_3 (mg/g $min^{1/2}$) are the rate constant of the pseudo-first order, the pseudo-second-order rate constant and the diffusion rate constant, respectively; C (mg/g) is a constant.

The percent relative deviation modulus, P, as shown in Eq. (11) was used to test the goodness of fit of the pseudo-first-order, pseudo-second-order and intraparticle kinetic models (Padilla-Ortega et al. 2014).

$$P\% = 100 \times \frac{1}{N}\sum_{i=1}^{N}\left|\frac{Q_{e(exp)} - Q_{e(cal)}}{Q_{e(exp)}}\right|_i \quad (11)$$

where $Q_{e(exp)}$ and $Q_{e(cal)}$ are the experimental and calculated equilibrium adsorption capacity (mg/g) of the adsorbent, respectively. N is the number of measurements. It was demonstrated that the adsorption process follows pseudo-second-order expression as shown in Eq. (9). The plots of t/Q_t versus time are linear. The values of Q_e and k_2 for the two adsorbents can be calculated from the slopes and intercepts of these pseudo-second-order kinetic plots by using Eq. (9). When $t \rightarrow 0$, the initial adsorption rate, h, can be defined as Eq. (12) (Shuang et al. 2015).

$$h = k_2 Q_e^2 \quad (12)$$

The values of the rate constant, the adsorption capacity, the initial adsorption rate, the correlation coefficients and the $P\%$ are presented in Table 2.

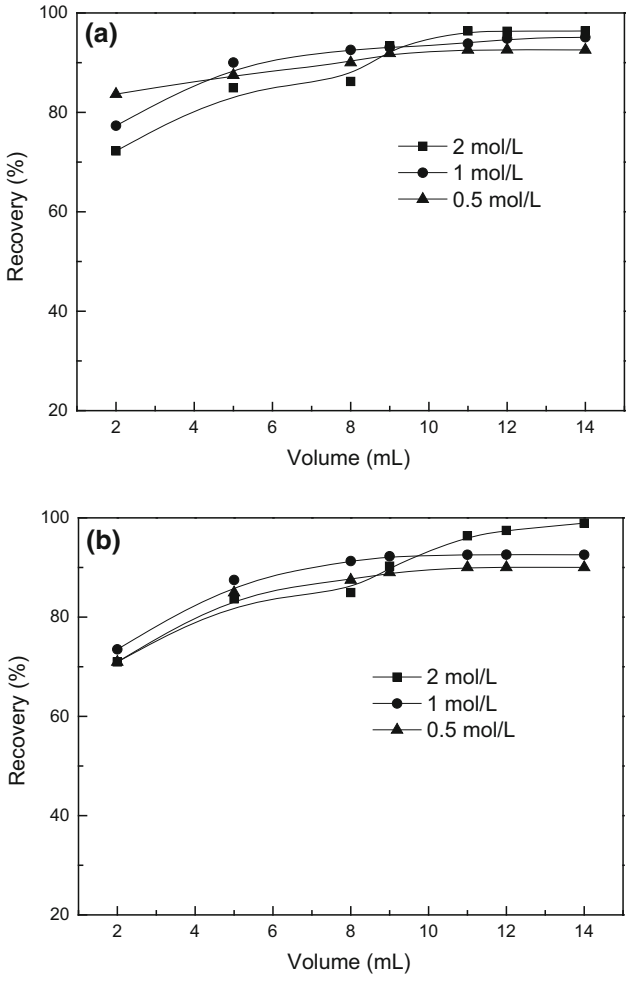

Fig. 6 Effect of concentrations and volumes of HCl on the recovery of 2,4-DNP from $SilprP_3NImBr$ (**a**) and $SilprSP_3NImBr$ (**b**)

Dynamic adsorption, elution and reuse

According to the batch experimental results, HCl was used as elution agent. The elution conditions were investigated by using various concentrations and volumes of HCl for the desorption of retained 2,4-DNP. The experimental results were presented in Fig. 6. It can be seen from this figure that the recovery of 2,4-DNP increased with the increase in the volume of HCl and the recovery was more than 90 % with 8 mL of 1 mol/L HCl in spite of the type of adsorbents. Regenerability is an important factor for an effective adsorbent. When 8 mL of 1 mol/L HCl was used as eluent, adsorption–elution cycles were also carried out. The experimental results show that the recovery of 2,4-DNP did not decrease significantly within at least eight adsorption–elution cycles, which indicated that the two adsorbents possess good stability and potential regeneration ability.

Comparison with other adsorbents

The adsorption capacities of 2,4-DNP onto $SilprP_3NImBr$ and $SilprSP_3NImBr$ were 91.74 and 51.81 mg/g, respectively, which were significantly larger than that of bare silica (0.48 mg/g). Compared with the other adsorbents reported in the literature such as AP-55 (280 mg/g), granular activated carbon (32.9 mg/g), charcoal activated powder (187.1 mg/g) (Daifullah and Girgis 1998), activated carbon fibers (418.3 mg/g) (Liu et al. 2010), carbon nanospheres (32.8 mg/g) (Lazo-Cannata et al. 2011), yellow bentonite (9.9 mg/g) (Yaneva and Koumanova 2006), MIP-SiO_2 (15.6 mg/g) (Luo et al. 2008), olive wood (5.9 mg/g) (El-Sheikh et al. 2013) and cotton cellulose C2 (11.2 mg/g) (Vismara et al. 2009), it can be concluded that the two adsorbents can be used to remove 2,4-DNP from aqueous solutions as effectively as the other adsorbents. Further compared with the previously synthesized imidazole-modified silica adsorbents in our group such as SilprImCl (33.3 mg/g), $SilprM_1ImCl$ (33.9 mg/g), $SilprM_2ImCl$ (35.9 mg/g), $SilprM_4ImCl$ (37 mg/g) and $SilprM_1M_2ImCl$ (35.3 mg/g) (Wang et al. 2013a, b), it is apparent that $SilprP_3NImBr$ and $SilprSP_3NImBr$ show adsorption ability superior to the other imidazole-modified silica adsorbents reported in the literature and is more effective for the adsorption of 2,4-DNP, which may be attributed to the additional electrostatic interactions between the amino groups and 2,4-DNP molecules. In addition, the other advantage of the two adsorbents is to keep a stable adsorption capacity for 2,4-DNP in the pH range of 4.0–9.0. Though there are significant differences in the structures of these adsorbents, experimental results show that these adsorbents are of primary anion-exchange and electrostatic nature.

This should be attributed to the underlying physicochemical properties of these adsorbents.

Conclusion

Based on the experimental results, it is clear that the two types of adsorbents are of primary anion-exchange and electrostatic nature. Amino groups play an important role in enhancement of adsorption capacities of 2,4-DNP onto $SilprP_3NImBr$ and $SilprSP_3NImBr$ by the additional electrostatic interactions between the amino groups and 2,4-DNP molecules. The linker between the silica and the imidazole ring affects the adsorption capacity of $SilprP_3NImBr$ and $SilprSP_3NImBr$. The adsorption capacities achieved with $SilprP_3NImBr$ using the propyl as the linker were higher than those of $SilprSP_3NImBr$ using the propyl sulfide as the linker. The adsorption capacities remained constant in the pH range of 4.0–9.0 and increased with an increase in the initial concentration. The experimental data were fitted well with the linear form of Langmuir model and the adsorption kinetics followed a pseudo-second-order model. The two adsorbents could be regenerated and reused eight times at least by washing with HCl without any appreciable loss of their original adsorption capacity. Such amino functionalized imidazole-modified silica adsorbents exhibit a potential candidate for the removal and recovery of 2,4-DNP from water. It should also be pointed out that the inhibitory effect of anions might be the potential drawback which limits the full application of the two adsorbents to treat wastewaters. Further work is underway in our laboratory to overcome the inhibitory effect by novel ionic liquid-modified silica adsorbents where the anions and cations of the ionic liquids were co-immobilized on the silica. When production in large scale starts and the price of ionic liquids drops significantly, the application of ionic liquid-modified silica adsorbents would be promoted.

Acknowledgments The financial support provided by National Natural Science Foundation of China (No. 21107022), the Key Scientific Research Project of Higher Education of Henan Province of China (No. 15A610007) and the Education Department of Henan Province of China (No. 2010GGJS-067) are gratefully acknowledged.

References

Arrigo R, Havecker M, Wrabetz S, Blume R, Lerch M, McGregor J, Parrott EPJ, Zeitler JA, Gladden LF, Knop-Gericke A, Schlogl R, Su DS (2010) Tuning the acid/base properties of nanocarbons by functionalization via amination. J Am Chem Soc 132:9616–9630

Ayusheev AB, Taran OP, Seryak IA, Podyacheva OY, Descorme C, Besson M, Kibis LS, Boronin AI, Romanenko AI, Ismagilov ZR, Parmon V (2014) Ruthenium nanoparticles supported on nitrogen-doped carbon nanofibers for the catalytic wet air oxidation of phenol. Appl Catal B Environ 146:177–185

Barrett EP, Joyner LG, Halenda PP (1951) The determination of pore volume and area distributions in porous substances. I. Computations from nitrogen isotherms. J Am Chem Soc 73:373–380

Bi W, Row KH (2010) Novel bi-functional amino-imidazolium silica confined stationary phase for liquid chromatography. J Liq Chromatogr Relat Technol 33:1459–1475

Chao Y, Zhu W, Wu X, Hou F, Xun S, Wu P, Ji H, Xu H, Li H (2014) Application of graphene-like layered molybdenum disulfide and its excellent adsorption behavior for doxycycline antibiotic. Chem Eng J 243:60–67

Chaudhary N, Balomajumder C (2014) Optimization study of adsorption parameters for removal of phenol on aluminum impregnated fly ash using response surface methodology. J Taiwan Inst Chem Eng 45:852–859

Daifullah AAM, Girgis BS (1998) Removal of some substituted phenols by activated carbon obtained from agricultural waste. Water Res 32:1169–1177

Duarte KR, Justino C, Panteleitchouk T, Zrineh A, Freitas AC, Duarte AC, Rocha-Santos TAP (2014) Removal of phenolic compounds in olive mill wastewater by silica–alginate–fungi biocomposites. Int J Environ Sci Technol 11:589–596

El-Sheikh AH (2014) Partial pyrolysis of olive wood to improve its sorption of chlorophenols and nitrophenols. Int J Environ Sci Technol 11:1459–1472

El-Sheikh AH, Newman AP, Said AJ, Alzawahreh AM, Abu-Helal MM (2013) Improving the adsorption efficiency of phenolic compounds into olive wood biosorbents by pre-washing with organic solvents: equilibrium, kinetic and thermodynamic aspects. J Environ Manage 118:1–10

Feng YB, Hong L, Liu AL, Chen WD, Li GW, Chen W, Xia XH (2015) High-efficiency catalytic degradation of phenol based on the peroxidase-like activity of cupric oxide nanoparticles. Int J Environ Sci Technol 12:653–660

Fu J, He Q, Wang R, Liu B, Hu B (2011) Comparative study of phenol compounds adsorption on mesoporous sieves with different degrees of modification. Colloids Surf A Physicochem Eng Asp 375:136–140

Gimbert F, Morin-Crini N, Renault F, Badot PM, Crini G (2008) Adsorption isotherm models for dye removal by cationized starch-based material in a single component system: error analysis. J Hazard Mater 157:34–46

Guo W, Chen R, Liu Y, Meng M, Meng X, Hu Z, Song Z (2013) Preparation of ion-imprinted mesoporous silica SBA-15 functionalized with triglycine for selective adsorption of Co(II). Colloids Surf A Physicochem Eng Asp 436:693–703

Han H, Wang Q, Liu X, Jiang S (2012) Polymeric ionic liquid modified organic-silica hybrid monolithic column for capillary electrochromatography. J Chromatogr A 1246:9–14

Huang J, Yang L, Wu X, Xu M, Liu Y, Deng S (2013) Phenol adsorption on α, α′-dichloro-p-xylene (DCX) and 4,4′-bis(chloromethyl)-1,1′-biphenyl (BCMBP) modified XAD-4 resins from aqueous solutions. Chem Eng J 222:1–8

Hurwitz G, Pornwongthong P, Mahendra S, Hoek EMV (2014) Degradation of phenol by synergistic chlorine-enhanced photo-assisted electrochemical oxidation. Chem Eng J 240:235–243

Khdary NH, Ghanem MA, Merajuddine MG, Manie FMB (2014) Incorporation of Cu, Fe, Ag, and Au nanoparticles in mercapto-silica (MOS) and their CO_2 adsorption capacities. J CO_2 Util 5:17–23

Kotadia DA, Soni SS (2012) Silica gel supported–SO_3H functionalised benzimidazolium based ionic liquid as a mild and effective catalyst for rapid synthesis of 1-amidoalkyl naphthols. J Mol Catal A Chem 353–354:44–49

Ladavos AK, Katsoulidis AP, Losifidis A, Triantafyllidis KS, Pinnavaia TJ, Pomonis PJ (2012) The BET equation, the inflection points of N_2 adsorption isotherms and the estimation of specific surface area of porous solids. Microporous Mesoporous Mater 151:126–133

Lazo-Cannata JC, Nieto-Márquez A, Jacoby A, Paredes-Doig AL, Romero A, Sun-Kou MR, Valverde JL (2011) Adsorption of phenol and nitrophenols by carbon nanospheres: effect of pH and ionic strength. Sep Purif Technol 80:217–224

Liu Q, Zheng T, Wang P, Jiang J, Li N (2010) Adsorption isotherm, kinetic and mechanism studies of some substituted phenols on activated carbon fibers. Chem Eng J 157:348–356

Liu B, Yang F, Zou Y, Peng Y (2014) Adsorption of phenol and p-nitrophenol from aqueous solutions on metal–organic frameworks: effect of hydrogen bonding. J Chem Eng Data 59:1476–1482

Lorenc-Grabowska E, Gryglewicz G, Diez MA (2013) Kinetics and equilibrium study of phenol adsorption on nitrogen-enriched activated carbons. Fuel 114:235–243

Luo W, Zhu L, Yu C, Tang H, Yu H, Li X, Zhang X (2008) Synthesis of surface molecularly imprinted silica micro-particles in aqueous solution and the usage for selective off-line solid-phase extraction of 2,4-dinitrophenol from water matrixes. Anal Chim Acta 618:147–156

Mahmoud ME (2011) Surface loaded 1-methyl-3-ethylimidazolium bis(trifluoromethylsulfonyl) imide [$EMIM^+Tf_2N^-$] hydrophobic ionic liquid on nano-silica sorbents for removal of lead from water samples. Desalination 266:119–127

Mahmoud ME, Al-Bishri HM (2011) Supported hydrophobic ionic liquid on nano-silica for adsorption of lead. Chem Eng J 166:157–167

Maroneze CM, Rahim A, Fattori N, da Costa LP, Sigoli FA, Mazali IO, Custodio R, Gushikem Y (2014) Electroactive properties of 1-propyl-3-methylimidazolium ionic liquid covalently bonded on mesoporous silica surface: development of an electrochemical sensor probed for NADH, dopamine and uric acid detection. Electrochim Acta 123:435–440

Mehrizad A, Zare K, Aghaie H, Dastmalchi S (2012) Removal of 4-chloro-2-nitrophenol occurring in drug and pesticide waste by adsorption onto nano-titanium dioxide. Int J Environ Sci Technol 9:355–360

Mousavi F, Pawliszyn J (2013) Silica-based ionic liquid coating for 96-blade system for extraction of aminoacids from complex matrixes. Anal Chim Acta 803:66–74

Păcurariu C, Mihoc G, Popa A, Muntean SG, Ianoş R (2013) Adsorption of phenol and p-chlorophenol from aqueous solutions on poly (styrene-co-divinylbenzene) functionalized materials. Chem Eng J 222:218–227

Padilla-Ortega E, Leyva-Ramos R, Mendoza-Barron J (2014) Role of electrostatic interactions in the adsorption of cadmium(II) from aqueous solution onto vermiculite. Appl Clay Sci 88–89:10–17

Qin G, Yao Y, Wei W, Zhang T (2013) Preparation of hydrophobic granular silica aerogels and adsorption of phenol from water. Appl Surf Sci 280:806–811

Qiu H, Wang L, Liu X, Jiang S (2009) Preparation and characterization of silica confined ionic liquids as chromatographic stationary phases through surface radical chain-transfer reaction. Analyst 134:460–465

Qiu H, Takafuji M, Liu X, Jiang S, Ihara H (2010) Investigation of π–π and ion–dipole interactions on 1-allyl-3-butylimidazolium ionic liquid-modified silica stationary phase in reversed-phase liquid chromatography. J Chromatogr A 1217:5190–5196

Shuang C, Wang J, Li H, Li A, Zhou Q (2015) Effect of the chemical structure of anion exchange resin on the adsorption of humic acid: behavior and mechanism. J Colloid Interface Sci 437:163–169

Srivastava VC, Swamy MM, Mall ID, Prasad B, Mishra IM (2006) Adsorptive removal of phenol by bagasse fly ash and activated carbon: equilibrium, kinetics and thermodynamics. Colloids Surf A Physicochem Eng Asp 272:89–104

Sun J, Chen Z, Ge M, Xu L, Zhai M (2013) Selective adsorption of Hg(II) by γ-radiation synthesized silica-graft-vinyl imidazole adsorbent. J Hazard Mater 244–245:94–101

Tian M, Row KH (2011) Separation of four bioactive compounds from Herba artemisiae scopariae by HPLC with ionic liquid-based silica column. J Anal Chem 66:580–585

Tian M, Bi W, Row KH (2013) Multi-phase extraction of glycoraphanin from broccoli using aminium ionic liquid-based silica. Phytochem Anal 24:81–86

Vafaeezadeh M, Hashemi MM (2014) Efficient fatty acid esterification using silica supported Brønsted acidic ionic liquid catalyst: experimental study and DFT modeling. Chem Eng J 250:35–41

Vala RMK, Tichagwa L, Dikio ED (2014) Evaluation of N-terminated siloxanes grafted onto lignocelluloses as adsorbent for the removal of phenol red from water. Int J Environ Sci Technol. doi:10.1007/s13762-014-0679-8

Velasco L, Ania C (2011) Understanding phenol adsorption mechanisms on activated carbons. Adsorption 17:247–254

Vidal L, Parshintsev J, Hartonen K, Canals A, Riekkola M (2012a) Ionic liquid functionalized silica for selective solid-phase extraction of organic acids, amines and aldehydes. J Chromatogr A 1226:2–10

Vidal L, Riekkola ML, Canals A (2012b) Ionic liquid-modified materials for solid-phase extraction and separation: a review. Anal Chim Acta 715:19–41

Vismara E, Melone L, Gastaldi G, Cosentino C, Torri G (2009) Surface functionalization of cotton cellulose with glycidyl methacrylate and its application for the adsorption of aromatic pollutants from wastewaters. J Hazard Mater 170:798–808

Wang F, Zhang Z, Yang J, Wang L, Lin Y, Wei Y (2013a) Immobilization of room temperature ionic liquid (RTIL) on silica gel for adsorption removal of thiophenic sulfur compounds from fuel. Fuel 107:394–399

Wang Z, Ye C, Li J, Wang H, Zhang H (2013b) Comparison and evaluation of five types of imidazole-modified silica adsorbents for the removal of 2,4-dinitrophenol from water samples with the methyl group at different positions of imidazolium ring. J Hazard Mater 147:955–966

Wiśniewski M, Terzyk AP, Gauden PA, Kaneko K, Hattori Y (2012) Removal of internal caps during hydrothermal treatment of bamboo-like carbon nanotubes and application of tubes in phenol adsorption. J Colloid Interface Sci 381:36–42

Yaneva Z, Koumanova B (2006) Comparative modelling of mono- and dinitrophenols sorption on yellow bentonite from aqueous solutions. J Colloid Interface Sci 293:303–311

Yang G, Chen H, Qin H, Feng Y (2014) Amination of activated carbon for enhancing phenol adsorption: effect of nitrogen-containing functional groups. Appl Surf Sci 293:299–305

Yousef RI, El-Eswed B, Al-Muhtaseb AH (2011) Adsorption characteristics of natural zeolites as solid adsorbents for phenol removal from aqueous solutions: kinetics, mechanism, and thermodynamics studies. Chem Eng J 171:1143–1149

Zhang W, Huang G, Wei J, Li H, Zheng R, Zhou Y (2012) Removal of phenol from synthetic waste water using Gemini micellar-enhanced ultrafiltration (GMEUF). J Hazard Mater 235–236:128–137

Zhang M, Liang X, Jiang S, Qiu H (2014) Preparation and applications of surface-confined ionic-liquid stationary phases for liquid chromatography. Trends Anal Chem 53:60–72

Zhou L, Meng X, Fu J, Yang Y, Yang P, Mi C (2014) Highly efficient adsorption of chlorophenols onto chemically modified chitosan. Appl Surf Sci 292:735–741

Zhu J, Xin F, Huang J, Dong X, Liu H (2014) Adsorption and diffusivity of CO_2 in phosphonium ionic liquid modified silica. Chem Eng J 246:79–87